Turkish Journal of Electrical Engineering & Computer Sciences

http://journals.tubitak.gov.tr/elektrik/

Research Article

Turk J Elec Eng & Comp Sci
(2018) 26: 1171 – 1179

doi:10.3906/elk-1711-50

A comparative study on different types of metamaterials for enhancement of microstrip patch antenna directivity at the Ku-band (12 GHz)

Bilal TÜTÜNCÜ[1,*], Hamid TORPİ[1], Bülent URUL[2]

[1]Department of Electronics and Communications Engineering, Faculty of Electrical & Electronics Engineering, Yıldız Technical University, Esenler, İstanbul, Turkey

[2]Department of Electronics and Automation, Vocational School of Technical Science, Süleyman Demirel University, Isparta, Turkey

Received: 06.11.2017 • **Accepted/Published Online:** 29.01.2018 • **Final Version:** 30.05.2018

Abstract: This paper proposes improving the directivity of microstrip patch antennas (MPAs) by using metamaterials. Four different metamaterial types are used as a flat lens in front of the MPA, respectively, which are tuned to 12 GHz (Ku-band) resonance frequency. Thus, it can be decided which metamaterial is more proper for antenna directivity enhancement at this band. One additional new metamaterial structure is proposed in this paper, which is called a Euro-shaped resonator, and other metamaterials used are the triangular split ring resonator, symmetrical ring structure, and split ring resonator. The permeability and permittivity of metamaterials are extracted from the S parameters by using a robust method. Microwave Studio by Computer Simulation Technology is used for modeling and simulation. The MPA and metamaterials are fabricated, and measurements are performed in the Yıldız Technical University RF and Microwave Laboratory. It is observed that measured results are in close agreement with the computer simulations.

Key words: Metamaterial, microstrip patch antenna, Ku-band, Euro-shaped resonator, triangular split ring resonator, symmetrical ring structure, split ring resonator

1. Introduction

Materials are classified in four groups with respect to permittivity ε and permeability μ. The materials that have both positive ε and positive μ ($\varepsilon > 0$, $\mu > 0$) are called double-positive materials. Most naturally occurring media (e.g., dielectrics) are considered in this group. If a material has negative ε and positive μ ($\varepsilon < 0$, $\mu > 0$), it is called an epsilon-negative material. In certain frequency regimes, many plasmas exhibit these characteristics. If a material has positive ε and negative μ ($\varepsilon > 0$, $\mu < 0$) it is called a mu-negative material and some gyrotropic materials show these properties. If both the permeability (μ) and the permittivity (ε) parameters are set negative at the same frequency, this class of materials is called double-negative (DNG) material or metamaterial (MM) [1]. MMs are not found in nature but they can be artificially designed. These are the materials that provide their properties from their structure rather than the material of which they are composed.

In 1968, Veselago presented that, if both the electric permittivity ε and the magnetic permeability μ of a material are negative, then negative refraction can occur and this inverse refraction causes focusing [1]. If electromagnetic waves can be focused instead of omnidirectional transmission, then the directivity and thus the

*Correspondence: bilal1334@gmail.com.tr

gain can be increased [2]. Therefore, in order to improve antenna gain and directivity, MM structures are used on antenna substrates [3,4], or on direct antenna geometry [5,6] or as lenses [7,8].

In a study by Zani et al., a new antenna was developed by using a single-cell split ring resonator (SRR) MM substrate for a circular microstrip patch antenna. It was shown that the gain of the circular patch antenna can be increased from 4.17 dBi to 5.66 dBi, even though the size of the new antenna is smaller than the antenna without MM [5]. In another study by Adel et al was proved that single and multiple layers of omega-shaped MMs that are formed as lenses at a half-wave distance oriented MM can improve the gain of a compact microstrip antenna at 10.5 GHz. The effects of using one or two MM layers and distances of MM layers to patch antenna were also compared [7].

In this study, a new MM structure (Euro-shaped structure, ESR) is designed and produced. The three best known MMs, the triangular split ring resonator (TSRR), the symmetrical ring structure (SRS), and the SRR, are then designed and fabricated. The antenna directivities of these four different MM structures are compared at 12 GHz. A rectangular microstrip patch antenna (MPA) is used as a reference antenna and fed by a microstrip line. Utilizing the relevant formulas and with a few CST experiments, the operating frequency of the rectangular MPA is set to 12 GHz. For impedance matching, two adjacent parallel slits are extended until the desired resonance input impedance value (50 Ω) is achieved [9]. Then the MM structures are used as a flat lens in front of the rectangular MPA.

Modeling, scaling, and simulations are done by CST Studio Suite. The robust method introduced in [10] is utilized to extract the effective permittivity and permeability from S parameters to analyze whether the structures are DNG at 12 GHz or not. Prototyping and laboratory measurements are made in the RF and Microwave Laboratory of the Electronics and Communications Department of Yıldız Technical University. Initial results of the reference antenna are obtained without using the MM lens. Then each MM single layer consisting of a 2 $\times$ 2 unit cell is placed at a distance of half wavelength of the MPA as a flat lens and results are obtained. It is observed that each MM increases the directivity but the most enhancement is with the ESR (the newly designed MM structure), with a 2.46 dB increase.

2. Reference MPA modeling, simulation, and measurement

MPAs are easy to fabricate, to feed, and to use in an array or incorporate with other microstrip circuit elements. Furthermore, dual frequency antennas can be made easily and they are compatible with microwave monolithic integrated circuit design, and feed lines and matching networks are fabricated simultaneously with the antenna structure [11]. However, microstrip antennas also have some limitations compared to conventional microwave antennas, such as low gain and low directivity. Appropriate designs can be used to solve these problems. Lower gain and lower power handling constraints can be overcome through an array configuration, but the two main disadvantages of this method come from the feeding of each antenna and also from the coupling between each element. A suitable model to eliminate these two disadvantages is to use a separate superstrate structure. For this purpose, four different MM structures are used, compared, and presented in this study.

Initially a MPA is modeled and simulated. A copper-coated Rogers RO4350B is used as a dielectric substrate. The relative dielectric constant (ε_r) is 3.48, the dielectric loss tangent is 0.0037, and the thickness is 0.762 mm. The dimensions of the patch antenna for 12 GHz resonance frequency are given in Figure 1. The reference MPA is then fabricated depending on these dimensions.

It is well known that circularly polarized EM waves could be constructed by superposition of a linear polarized EM wave of equal amplitude by differing in phase by 90°. Thus, analyzing our antenna for linear polarization is sufficient for our purposes.

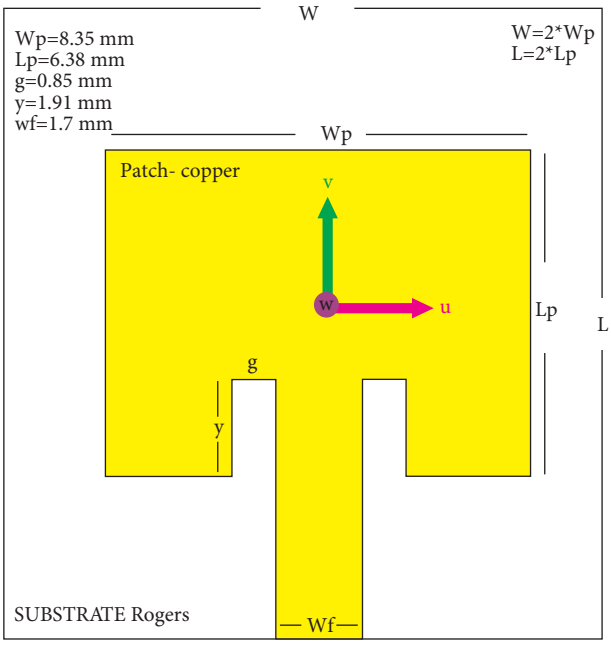

Figure 1. Reference MPA antenna shape and dimensions.

Finally, the S_{11} curves of the MPA according to the measurement and simulation results were drawn as shown in Figure 2. In order to compare the increase in the directivity, the simulation and measurement results are taken separately and the far-field radiation pattern of the MPA is drawn for 12 GHz. The peak directivity is found as 4.66 dBi/4.32 dBi (simulation/measurement), as shown in Figure 3. Furthermore, according to the simulation results, the half power beam-width (HPBW) is 93.1°.

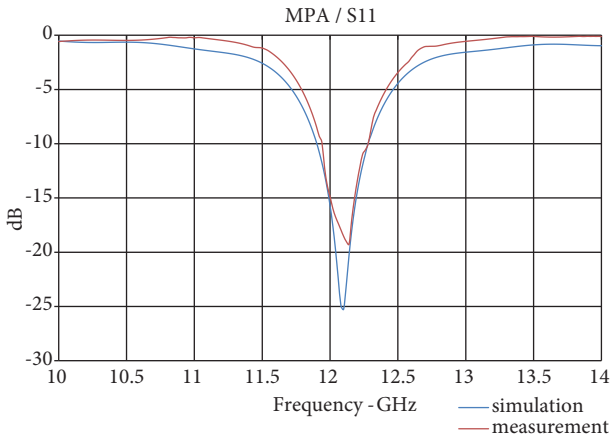

Figure 2. S_{11} curve of the rectangular MPA.

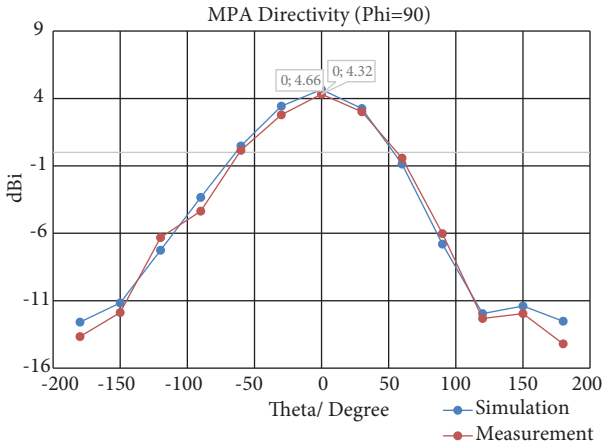

Figure 3. Radiation pattern of the rectangular MPA.

3. Different MM unit cell designs

The TSRR, SRS, SRR, and ESR structures are designed and fabricated by the LPKF ProtoMat S63 in-house prototyping machine. For each MM unit cell, the same substrates with predefined characteristics and dimensions are used for a fair comparison.

The simulation setup is designed similar to the free space dielectric measurement setup. This free space model requires electromagnetic radiation in TEM mode. For that reason, electromagnetic waves within the metamaterial are excited in TEM mode and the simulation setup is similar to the material placed in a waveguide environment that propagates in the Z-axis. The boundary conditions of the program are set so that the perfect electrical conductor is along the X-axis and the perfect magnetic conductor is along the Y-axis. Owing to these boundary conditions, the MM unit cell is excited by TEM waves. For high-frequency measurements, the simulations are made in the time domain method since it is considered to be the best in terms of speed [12].

To obtain the media parameters (ε and μ) from the S parameters, we have used the robust method, and S_{11} and S_{21} values are taken for the relevant frequency values. Then the refractive index n and the impedance z are calculated with the help of the equations given in [10]. Then ε_{eff} and μ_{eff} are computed from refractive index n and impedance z [13] by Eqs. (1) and (2). In this section, we have investigated whether the materials are DNG or not, so we are only concerned with the transmitted part of the electromagnetic waves. Thus, the imaginary parts that represent the loss energy are ignored [14].

$$\varepsilon_{eff} = \frac{n}{z} \tag{1}$$

$$\mu_{eff} = nz \tag{2}$$

4. Triangular split ring resonator (TSRR)

In this structure, there are two nested triangles that are symmetrical to each other at the front side of the TSRR and a strip for negative permittivity on the back side. The gap of the outer triangle is at its base and the gap of the inner triangle is at exactly 180° symmetrical to the gap of the outer triangle [15]. Both triangles are designed to be isosceles.

In CST, a k multiplier is defined in the parameter list and the results are obtained for each k value; thus, the TSRR structure is optimized. The shape and the dimensions of the TSRR from the front side are shown in Figure 4. The width of the back strip is 0.4 mm and the length of this strip is 4 mm. The curves of ε_{eff} and μ_{eff} are as shown in Figure 4. As seen, both ε_{eff} and μ_{eff} values are negative at 12 GHz $(\varepsilon_{eff} = -0.8, \mu_{eff} = -3.9)$.

4.1. Symmetrical ring structure (SRS)

This MM consists of two symmetrical rectangular rings along the X-axis at the front side and a copper conductor strip extending in the Y-plane along the substrate at the back side. There is also a gap in each ring [12,16]. The shape and dimensions of the front side of the SRS structure and ε_{eff} and μ_{eff} curves are shown in Figure 5. The width of the back strip is 0.4 mm and the length of this strip is 5 mm. As seen, values of ε_{eff} and μ_{eff} are negative at 12 GHz. $(\varepsilon_{eff} = -1.6, \mu_{eff} = -2.1)$.

4.2. Split ring resonator (SRR)

The SRR is the first designed MM structure [17] and it is the most popular. On the front side of the substrate, there are two nested square rings that have symmetrical gaps to each other to achieve negative μ and on the back side there is a copper strip to achieve negative ε [17,18]. The length and width of the strip on back side are 5.6 mm and 0.4 mm, respectively. The front shape and dimensions of the SRR structure and the ε_{eff} and μ_{eff} curves are shown in Figure 6. As seen, $\varepsilon_{eff} = -0.2033$ and $\mu_{eff} = -0.4078$ at 12 GHz.

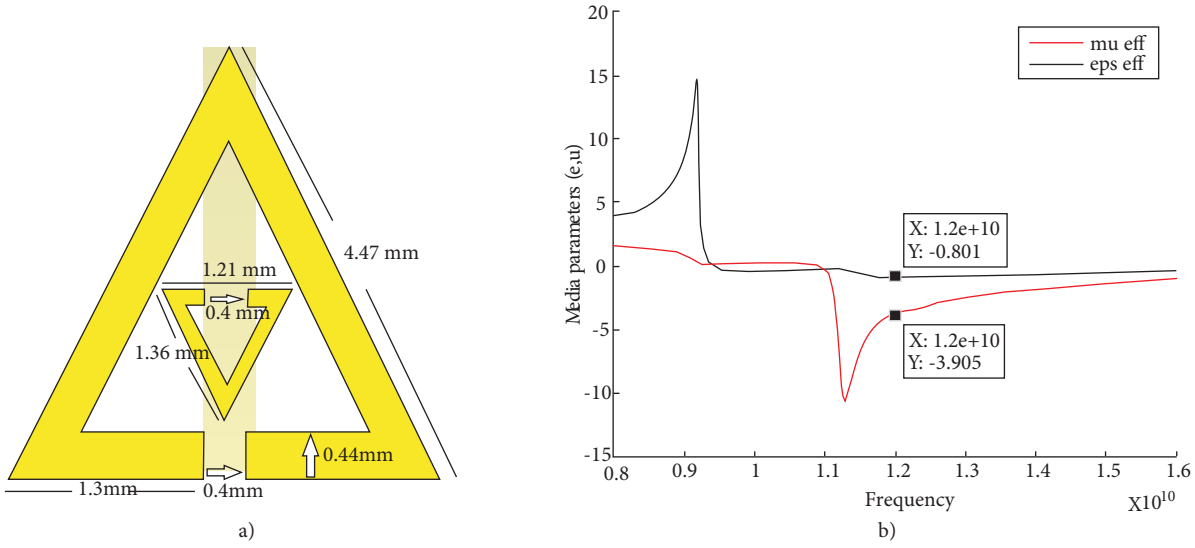

Figure 4. TSRR: a) shape, b) media parameters (μ, ε).

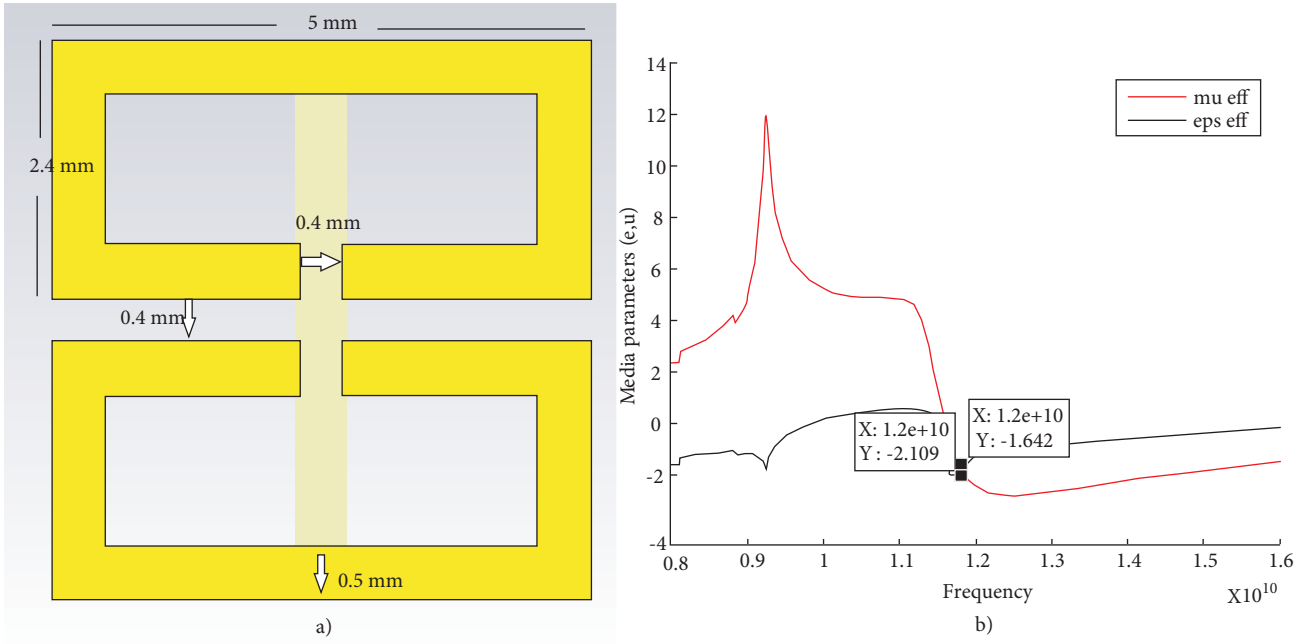

Figure 5. SRS: a) shape, b) media parameters (μ, ε).

4.3. Euro-shaped resonator (ESR)

This newly designed MM has two symmetrical crescent-shaped structures and there is a single dashed line between these two structures to increase the capacitive effect. The length and width of the strip on the back side are 4 mm and 0.3 mm, respectively. The shape and dimensions of the ESR structure from the front side and the ε_{eff} and μ_{eff} curves are shown in Figure 7. As seen, $\varepsilon_{eff} = -1.33$ and $\mu_{eff} = -2.18$ at 12 GHz.

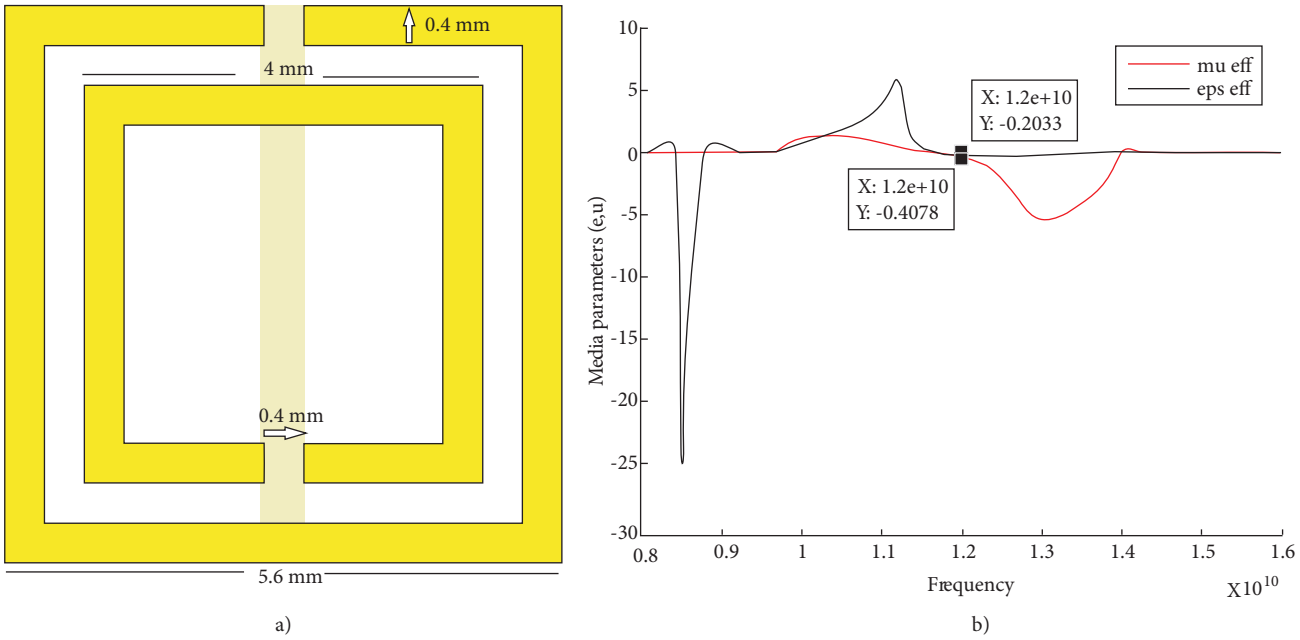

Figure 6. SRR: a) shape, b) media parameters (μ, ε).

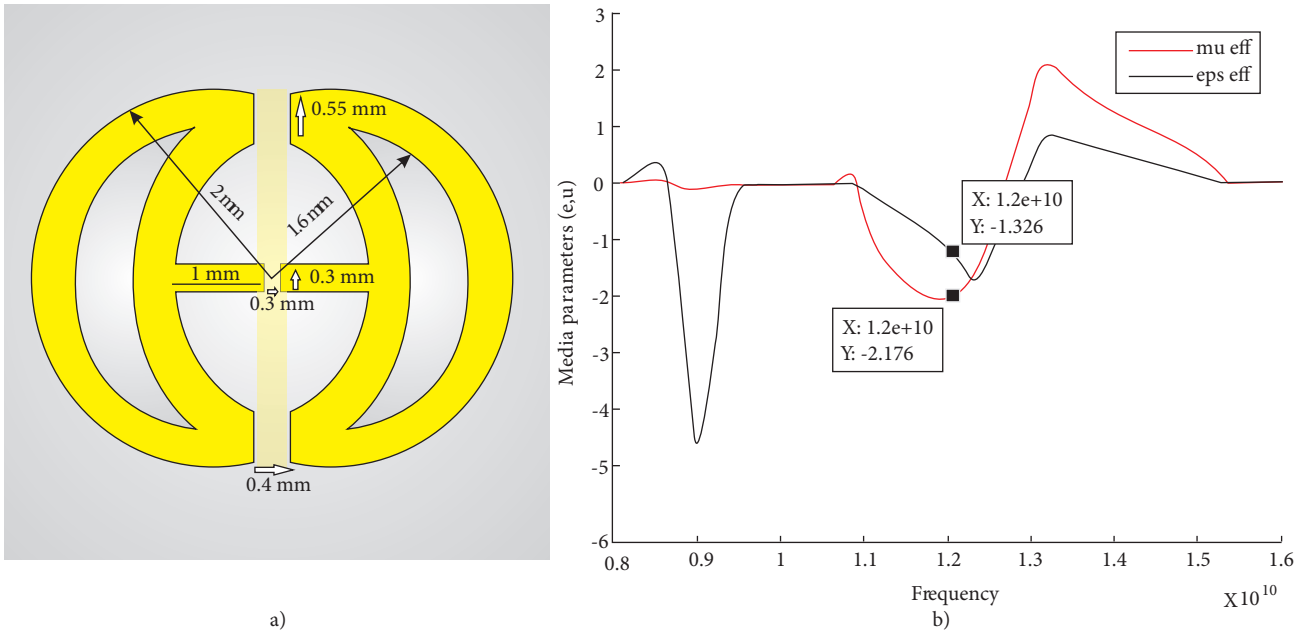

Figure 7. ESR: a) shape, b) media parameters (μ, ε).

5. Use of MM as lens

MM unit cells whose effective parameters are confirmed to be negative at 12 GHz have to be converted into a periodic structure to use as a lens for a significant increase. It is not desirable to increase the antenna size while increasing the antenna directivity. Thus, the size of the lens layers are chosen between the dimensions of the patch and the ground plane of the MPA. Therefore, parametric studies are carried out in different quantities of the unit cells to obtain optimal return loss and optimal radiation parameters in these limitations and a 2

× 2 periodic structure of 12 mm × 12 mm dimensions is noted as optimal so the fabrication of MMs is done according to this. The top view and bottom view of the fabricated MM lens structures are shown in Figure 8. The MM lens can be used as one layer or more [18]. For a compact design, we used only a one-layer MM structure instead of a multilayer structure.

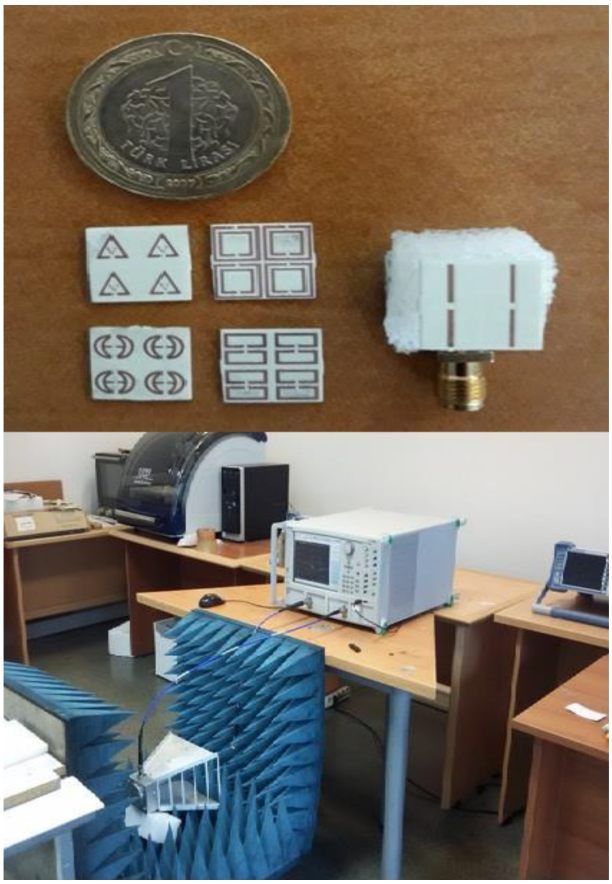

Figure 8. Photograph of fabricated prototype of MMs and measurement setup.

6. Results and discussion

Each type of MM with 2 × 2 periodic structure is used as a lens in front of the reference MPA and the simulation and measurement results are obtained. The radiation pattern of each proposed antenna is measured using the measurement setup given in Figure 8.

Figure 9 shows S_{11} curves and Figure 10 shows far-field directivity patterns of the MPA with MM lens structures at 12 GHz. Enhancements of the MPA directivity, HPBW, and change in bandwidths are given in the Table.

As can be seen, the most directive gain enhancement is with the ESR (the newly designed MM structure) with a 2.46 dB increase. The resonance behavior of MMs is due to capacitive and inductive elements (cavities, slits, and rings) of their geometries that cause very high positive and high negative magnetic permeability values [2]. The ESR geometry has more capacitive and inductive elements than the others in the same area dimensions. We can say that this may be the reason why the directivity increase of the MPA with the ESR is greater than others.

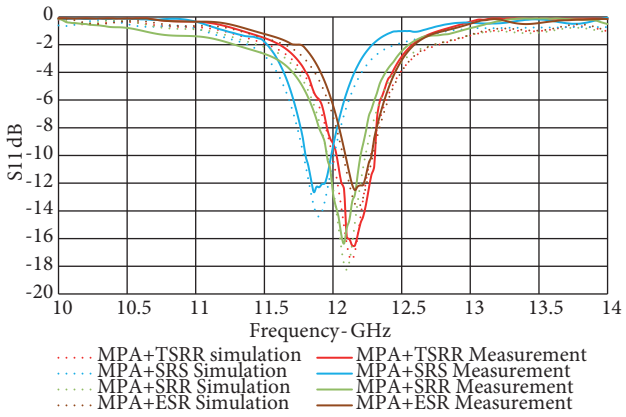

Figure 9. S_{11} curves of the MPA with MMs.

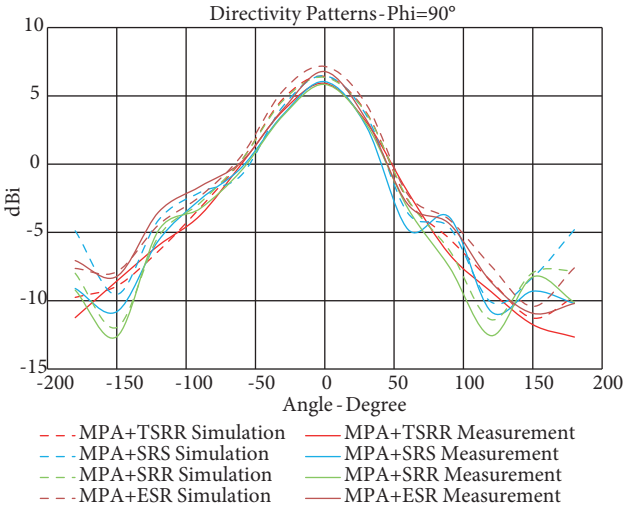

Figure 10. Directivity radiation patterns of the MPA with MMs.

Table. Simulation and measurement results of directivity, HPBW, and bandwidth.

					Comparison of antenna parameters of MPA + MM and without MM		
		Directivity dBi	HPBW degree	Bandwidth MHz	Directivity improvement (dB)	HPBW difference (degrees)	Bandwidth difference (MHz)
Only MPA	Sim.	4.66	93°	340			
	Meas.	4.32		320			
MPA+ TSRR	Sim.	6.42	72°	260	1.76	–21°	–80
	Meas.	5.92		260	1.60		–60
MPA + SRS	Sim.	6.47	66°	200	1.81	–27°	–140
	Meas.	6.04		180	1.72		–160
MPA + SRR	Sim.	6.36	72°	260	1.70	–21°	–80
	Meas.	5.84		240	1.52		–80
MPA + ESR	Sim.	7.16	69°	200	2.51	–24°	–140
	Meas.	6.78		180	2.46		–140

When directivity increases, the bandwidth decreases, as expected. Moreover, the decrease in the HPBW is evidence of the enhancement of directivity in the radiation pattern. Consequently, the proposed antenna systems are more appropriate for studies that require high antenna directivity.

7. Conclusion

In this study, four differently shaped MM structures are used separately as flat lenses to increase the directivity of the reference MPA and compared. According to the measurement results at 12 GHz, the best improvement was achieved by a new MM array called ESR with an increase of 2.46 dB. The MPA directivity can be increased even more by using two or more ESR layers, but in this case the size of the antenna system will increase and

this is undesirable. The measurement results are slightly different from the simulation results. It is thought that this difference is due to media losses and fabrication defects.

Acknowledgment

I would like to thank to Prof Dr Tülay Yıldırım and research assistants Onurcan Kurban and Alper Çalışkan for their help and support in PCB prototyping of the MPA and MMs by LPKF.

References

[1] Veselago VG. The electrodynamics of substances with simultaneously negative values of and μ. Sov Phys Uspekhi 1968; 10: 509-514.

[2] Pendry JB. Negative refraction makes a perfect lens. Phys Rev Lett 2000; 85: 3966-3969.

[3] Shafique MF, Qamar Z, Riaz L, Saleem R, Khan S. Coupling suppression in densely packed microstrip arrays using metamaterial structure. Microw Opt Techn Let 2015; 57: 759-763.

[4] Amanatiadis S, Karamanos T, Kantartzis N. Radiation efficiency enhancement of graphene THz antennas utilizing metamaterial substrates. IEEE Antenn Wirel Pr 2017; 16: 2054-2057.

[5] Zani MZM, Jusoh MH, Sulaiman AA, Baba NH, Awang RA, Ain MF. Circular patch antenna on metamaterial. In: IEEE 2010 Electronic Devices, Systems and Applications Conference; 11–14 April 2010; Kuala Lumpur, Malaysia. New York, NY, USA: IEEE. pp. 313-316.

[6] Xiong H, Hong J, Tan M, Li B. Compact microstrip antenna with metamaterial for wideband applications. Turk J Electr Eng Co 2013; 21: 2233-2238.

[7] Adel BA, Ahmed AI. Metamaterial enhances microstrip antenna gain. Microwaves RF 2016; 7: 46-50.

[8] Li D, Szabo Z, Qing X, Li E, Chen ZN. A high gain antenna with an optimized metamaterial inspired superstrate. IEEE T Antenn Propag 2012; 12: 6018-6023.

[9] Balanis CA. Antenna Theory: Analysis and Design. 2nd ed. New York, NY, USA: John Wiley and Sons, 1997.

[10] Chen X, Grzegorcezyk TM, Wu BI, Pacheco J, Kong JA. Robust method to retrieve the constitutive effective parameters of metamaterials. Phys Rev E 2004; 70: 1-7.

[11] İmeci ST. E- and H-shaped high gain patch antennas. Microw Opt Techn Let 2015; 57: 1395-1401.

[12] Wu BI, Wang W, Pacheco J, Chen X, Grzegorczyk T, Kong JA. A study of using metamaterials as antenna substrate to enhance gain. Prog Electromagn Res 2005; 51: 295-328.

[13] Numan A, Sharawi M. Extraction of material parameters for metamaterials using a full-wave simulator. IEEE Antenn Propag M 2013; 5: 202-211.

[14] Çakır M, Koçkal NU, Özen Ş, Kocakuşak A, Helhel S. Investigation of electromagnetic shielding and absorbing capabilities of cementitious composites with waste metallic chips. J Microwave Power EE 2017; 51: 31-42.

[15] Sabah C. Tunable metamaterial design composed of triangular split ring resonator and wire strip for S- and C-microwave bands. Prog Electromagn Res 2010; 22: 341-357.

[16] O'Brien S, Pendry JB. Magnetic activity at infrared frequencies in structured metallic photonic crystals. J Phys-Condens Mat 2002; 14: 6383-6394.

[17] Smith DR, Vier DC, Kroll N, Schultz S. Direct calculation of permeability and permittivity for a left-handed metamaterial. Appl Phys Lett 2000; 77: 2246-2248.

[18] Bayındır M, Aydın K, Özbay E, Markos P, Soukoulis M. Transmission properties of composite metamaterials in free space. Appl Phys Lett 2002; 81: 120-122.